Acta Mech 198, 1–19 (2008)
DOI 10.1007/s00707-007-0523-z
Printed in The Netherlands

Acta Mechanica

Carrying capacity of edge-cracked columns under concentric vertical loads

K. Yazdchi[1], A. R. Gowhari Anaraki[2]

[1] Department of Mechanical Engineering, Amirkabir University of Technology (AUT), Tehran, Iran
[2] Department of Mechanical Engineering, Iran University of Science and Technology, Tehran, Iran

Received 16 April 2007; Accepted 8 October 2007; Published online 25 January 2008

Summary. This paper analyses the carrying capacity of edge-cracked columns with different boundary conditions and cross sections subjected to concentric vertical loads. The transfer matrix method, combined with fundamental solutions of the intact columns (e.g. columns with no cracks) is used to obtain the capacity of slender prismatic columns. The stiffness of the cracked section is modeled by a massless rotational spring whose flexibility depends on the local flexibility induced by the crack. Eigenvalue equations are obtained explicitly for columns with various end conditions, from second-order determinants. Numerical examples show that the effects of a crack on the buckling load of a column depend strongly on the depth and the location of the crack. In other words, the capacity of the column strongly depends on the flexibility due to the crack. As expected, the buckling load decreases conspicuously as the flexibility of the column increases. However, the flexibility is a very important factor for controlling the buckling load capacity of a cracked column. In this study an attempt was made to calculate the column flexibility based on two different approaches, finite element and J-Integral approaches. It was found that there was very good agreement between the flexibility results obtained by these two different methods (maximum discrepancy less than 2%). It was found that for constant column flexibility a crack located in the section of the maximum bending moment causes the largest decrease in the buckling load. On the other hand, if the crack is located just in the inflexion point at the corresponding intact column, it has no effect on the buckling load capacity. This study showed that the transfer matrix method could be a simple and efficient method to analyze cracked columns components.

1 Introduction

A no follower force is usually referred as an axial force with its direction remaining constant during the deformation of the structure and column buckling defined as the change of its equilibrium state from one configuration to another at a critical compressive load. However, stability represents one of the main problems in solid mechanics and must be controlled to ensure the safety of a structure against collapse. It has a crucial importance, especially for structural, aerospace, mechanical, nuclear, offshore and ocean engineering. Buckling is one of the fundamental forms of instability of column structures. The mathematical solutions for the critical buckling loads for columns under different boundary conditions subjected to no follower compression are well documented by

Correspondence: Kazem Yazdchi, Department of Mechanical Engineering, Amirkabir University of Technology (AUT), Tehran, Iran
e-mail: kyazdchi@gmail.com

Timoshenko and Gere [1]. Euler [2] introduced the concept of the critical load of an elastic column in detail in 1744.

Columns and compression members may usually contain various imperfections like cracks. Imperfections have been recognized for a long time and their effects on structural stability have been well investigated. Columns and other structural elements may also have real damage such as cracks. The cracks may develop from flaws due to applied cyclic loads, mechanical vibrations, aerodynamic loads, etc. It is obvious that crack causes a lower structural integrity and should be certainly taken into account in the stability, safety and vibration analysis of structures.

The rotational discontinuity of a cracked column at the crack location has been readily modeled in Ref. [3]. This model has been used for the dynamic analysis of a damaged structure, where the change in the flexibility of the beam due to a crack has been advocated. Liebowitz et al. [4] carried out experimental studies on the axial load carrying capacity of notched and unnotched columns. For notched columns, Liebowitz and Claus [5] proposed a theoretical failure criterion based on the stress intensity factor and fracture toughness. Okamura et al. [6] proposed a method to identify the compliance of a cracked column to a bending moment to study the load carrying capacity and fracture load of a slender column with a single crack. Anifantis and Dimarogonas [7] studied the buckling behavior of cracked columns subjected to follower and vertical loads. The buckling of cracked composite columns was also investigated by Nikpour [8]. Li [9] investigated the buckling of multi-step columns with an arbitrary number of cracks, taking into account the effect of shear deformations. However, research performed research to date on the stability of cracked columns lags far behind the performed research on uncracked ones. In this study, using the transfer matrix method and fundamental solution of intact columns, suggested in [10], a buckling analysis of slender prismatic columns of circular and rectangular cross section, with single and double nonpropagating edge cracks, is performed. The cracked section is replaced with a massless rotational spring whose flexibility is a function of the crack depth and the height of the cross section of the column. The spring flexibility is calculated based on two different approaches, finite element and J-Integral. A collapse failure criterion based on column flexibility is defined as an upper bound limit design control factor. Eigenvalue equations (buckling conditions) are obtained explicitly for columns with various common end conditions (namely: fixed–free, pinned–pinned, fixed–pinned, fixed–fixed), from second-order determinants. Taking a few example columns, these equations are solved and their smallest roots, which are the buckling loads of the columns, are determined. Moreover, the effects of the crack configuration factors are investigated and the results are given in the form of diagrams.

2 Material and geometry conditions

The dimensions used to define the geometries are shown in Fig. 1. They are the height of the rectangular cross section of the column, h, the width of the rectangular cross section of the column, b, the length of the column, L, and the depth of the crack, a. The diameter of the circular cross section of the column is h. The location of crack from the upper end of the column is measured with x_{c}. The depth of the crack is normalized with respect to the height of the rectangular cross section (or the diameter of the circular cross section), $\zeta = \frac{a}{h}$. The distance of the crack from the upper end of the column is normalized with the column length, $\beta = \frac{x_{\mathrm{c}}}{L}$. The concentric vertical load is applied at the upper end of the column as shown in Fig. 1. The mathematical model of the column is shown in Fig. 2, in which, after the local flexibility caused by crack is considered, the cracked section is represented by a massless rotational spring with local flexibility C. Let x denote, the coordinate along the length of the column with its origin at the upper end of the column. The positive direction

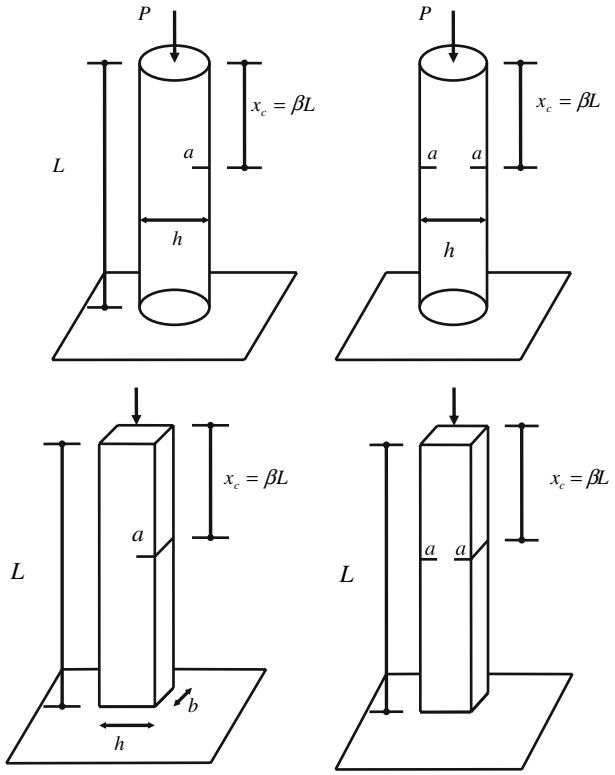

Fig. 1. Slender column with a non-propagating single and double edge crack

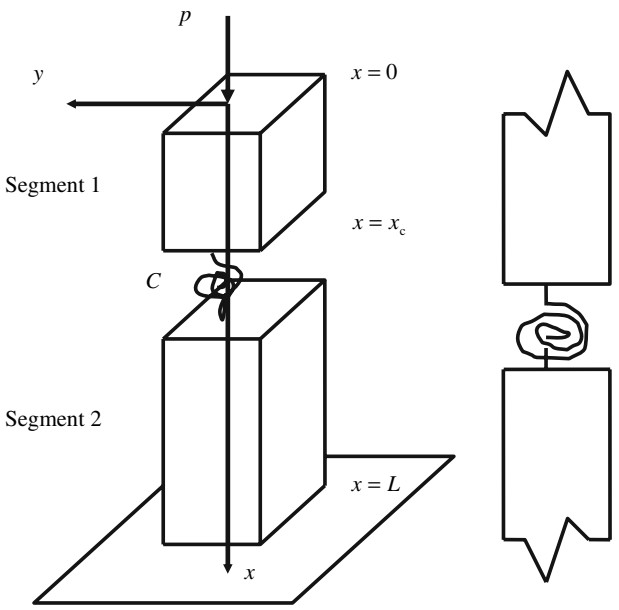

Fig. 2. A mathematical model for the rotational spring

of the deflection $y(x)$ of the column is defined leftward, as shown in Fig. 2. In this study, four common ends conditions, namely fixed–free, pinned–pinned, fixed–pinned and fixed–fixed, are used throughout the analysis, as shown in Fig. 3.

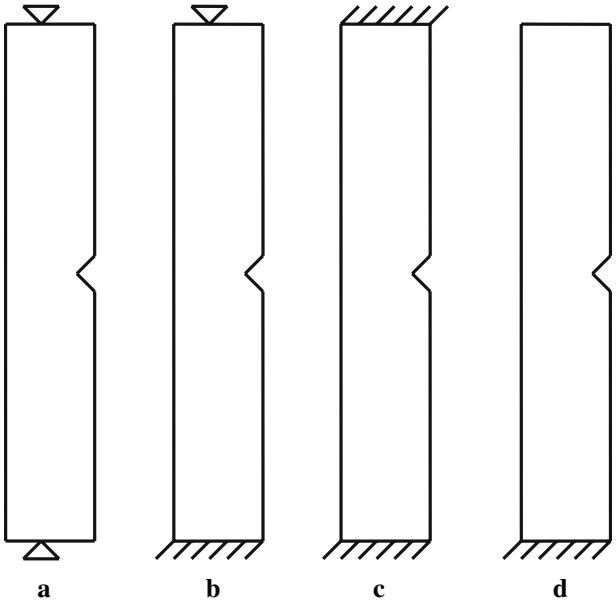

Fig. 3. The column end conditions.
a pinned-pinned **b** fixed-pinned
c fixed-fixed **d** fixed-free

3 Local flexibility of cracked column structure

A slender prismatic column with a circular and rectangular cross section, having a non-propagating single and double edge crack (or flaw like crack) are shown in Fig. 1. The cracked section is presented by a mass less rotational spring with flexibility C, where

$$M = k\Delta\theta \tag{1}$$

and

$$C = \frac{1}{k} = \frac{\Delta\theta}{M}. \tag{2}$$

This quantity is a function of the crack depth height and the flexural rigidity (EI) of the rectangular section of the column, and can be written as suggested in Ref. [11] as below:

$$C = \frac{h}{\mathrm{EI}} f(\zeta). \tag{3}$$

and for the circular cross section it is [12], [13]

$$C = \frac{D}{\mathrm{EI}} f(\zeta), \tag{4}$$

where $D = h$ is the diameter of the circular cross section and $f(\zeta)$ is called the local flexibility function.

In this study an attempt is made to calculate the local flexibility function of the column, using two different methods, finite element (FE) and J-Integral approach.

3.1 Prediction of the flexibility function using FEM

Finite element predictions have been obtained using the standard linear elastic fracture mechanics facilities within the Ansys suite of programs [14]. A typical mesh, using six- and eight-noded, reduced integration, plane stress, triangular and quadrilateral elements was used with the crack tip singularity

represented by moving nodes to the quarter point positions [14]. For a wide range of geometries considered, the angular displacement (i.e. $\Delta\theta$) is obtained by elastic linear fracture mechanics finite element analysis. The local flexibility, C, and local flexibility function, $f(\zeta)$, then are calculated using Eqs. (2) and (3), respectively. It is worth nothing that the finite element analysis is carried out for plane stress condition and for the unit value of the flexural rigidity, EI. The local flexibility functions are then modified by a correction factor of 1/EI, as indicated in Eq. (3) (see Fig. 4).

The variation of the local flexibility function, $f(\zeta)$, with the normalized crack depth, a/h, is shown in Fig. 5 for a prismatic column of rectangular cross section with a single non-propagating edge crack.

The variation of the local flexibility, C, with the normalized crack depth, $\zeta = a/h$, and different height of the cross section of the column is shown in Fig. 6 for a rectangular cross section column with a single edge crack.

The extensive range of the flexibility function, $f(\zeta)$, resulted from finite element analysis is used to obtain predictive equations using a statistical multiple nonlinear regression model. The accuracy of the model is measured using a multiple coefficient of determination, R^2, where $0 \leq R^2 \leq 1$. This coefficient is found to be greater than or equal to 0.995 for all cases considered in this study, demonstrating the quality of the model fit to the data.

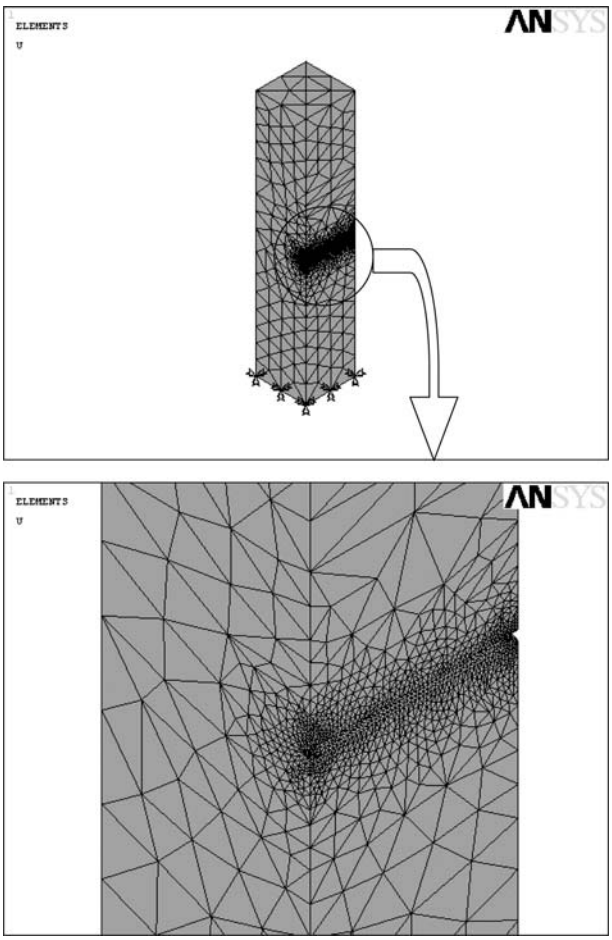

Fig. 4. A typical FE mesh

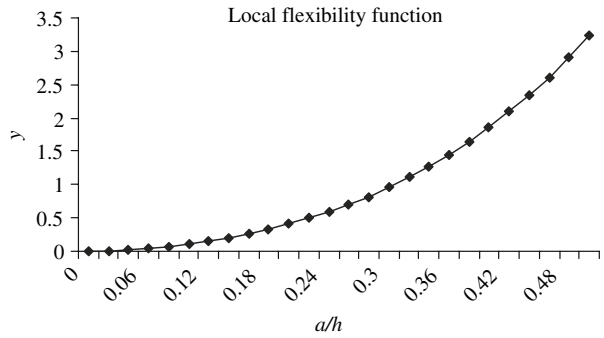

Fig. 5. The variation of $y = f(\zeta)$ with a/h for a single non-propagating edge cracked column with rectangular cross section

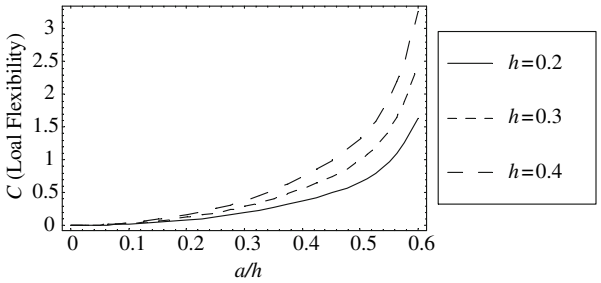

Fig. 6. The variation of C with ζ and h for a single non-propagating edge cracked column

The predictive equation $f(\zeta)$ for slender prismatic columns of rectangular cross section, with a single non-propagating edge crack, is predicted as

$$f(\zeta) = -0.0038 + 1.0459\zeta - 24.7331\zeta^2 + 450.54\zeta^3 - 2,800.2\zeta^4 + 8918.17\zeta^5 - 13907.2\zeta^6 + 8481.12\zeta^7. \tag{5}$$

Similar analyses are carried out for the prismatic column of rectangular cross section, with a double non-propagating edge crack. The variation of the flexibility function with normalized crack depth is shown in Fig. 7 for a column of rectangular cross section with a double edge crack. The finite element prediction of the flexibility function based on the statistical multiple non-linear regression model is as below:

$$f(\zeta) = -0.0017 + 0.5506\zeta - 20.8194\zeta^2 + 334.396\zeta^3 - 1833.32\zeta^4 + 5993.55\zeta^5 - 9600.42\zeta^6 + 6030.7\zeta^7. \tag{6}$$

The variation of the flexibility function with respect to the normalized crack depth is shown in Fig. 8 for the prismatic column of rectangular cross section, with a single and a double non-propagating edge crack. As it is expected, it can be seen that the double edge cracked column has a higher local flexibility than a single cracked column. These discrepancies become larger as the crack depth increases, or in other words, the predicted local flexibility for a double edge cracked column is more dominant when the crack depth increases.

In a similar way, the flexibility functions obtained from the finite element analysis, for the prismatic column of circular cross section with a single and a double edge crack, have been used to obtain useful equivalent prediction equations, using the statistical multiple non-linear regression method. These predictive equations for the local flexibility functions of the prismatic column of circular cross section, with a single and double non-propagating edge crack are presented in Eqs. (7) and (8), respectively, as follows:

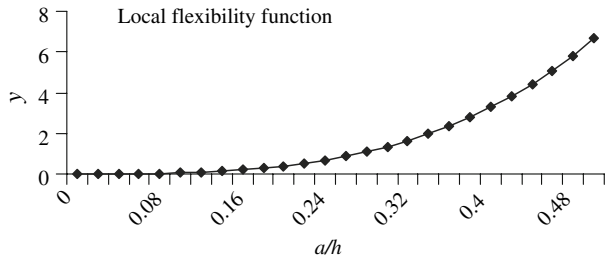

Fig. 7. The variation of $y = f(\zeta)$ with a/h for a double non-propagating edge cracked column with rectangular cross section

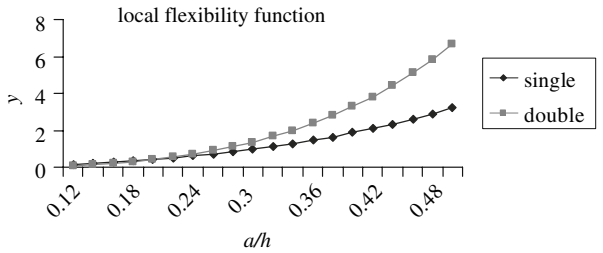

Fig. 8. The variation of $y = f(\zeta)$ with a/h for a single and a double non-propagating edge cracked component of rectangular cross section

$$f(\zeta) = 0.0007 + 0.3255\zeta - 8.4253\zeta^2 + 167.486\zeta^3 - 831.418\zeta^4 + 2266.89\zeta^5 - 3154.06\zeta^6 + 1852.87\zeta^7 \tag{7}$$

and

$$f(\zeta) = -0.0445 + 11.77\zeta - 393.721\zeta^2 + 4813.5\zeta^3 - 27314.8\zeta^4 + 79935\zeta^5 - 115803\zeta^6 + 66031.8\zeta^7. \tag{8}$$

The variation of local flexibility with respect to the crack depth is shown in Fig. 9 for the prismatic column of rectangular and circular cross sections, with a single and a double edge crack.

3.2 Prediction of the local flexibility function using the strain energy density function approach

The localized flexibility of the column can be calculated using the strain energy density function approach, suggested by Tada et al. in Ref. [15].

As an example, a section of a circular column containing a crack of depth a is shown in Fig. 10a. Figure 10b shows the cross section of the column section at the location of the transverse crack. The generalized displacement U_i in the i direction is obtained by utilizing Castigliano's theorem [16] as

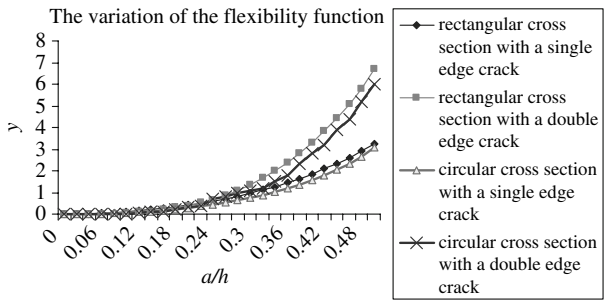

Fig. 9. The variation of the flexibility function with a/h for a single and a double edge crack

$$U_i = \frac{\partial}{\partial P_i} \int_0^a J(y) dy, \tag{9}$$

where P_i is the generalized force associated with U_i, and $J(y)$ is the strain energy density function given by Tada et al. [14] as

$$J(y) = \frac{1-\upsilon^2}{E} \left[\left(\sum_{i=1}^{m} K_{\mathrm{I}i} \right)^2 + \left(\sum_{i=1}^{m} K_{\mathrm{II}i} \right)^2 + (1+\upsilon) \left(\sum_{i=1}^{m} K_{\mathrm{III}i} \right)^2 \right], \tag{10}$$

where υ is Poisson's ratio, E is Young's modulus, and K_{ni} (where n = I, II, III) is the crack stress intensity factor for mode n due to P_i. m indicates the number of individual loads applied to the component. In this study $m = 1$, due to the only one concentric vertical load to the prismatic column. The stress intensity factors for a unit width strip containing a crack of depth a are evaluated according to

$$K_{ni} = \sigma_i \sqrt{\pi a} F_n \left(\frac{a}{h} \right), \tag{11}$$

where σ_i are the stresses due to the load P_i applied to the intact column (i.e., a column without any crack), $F_n\left(\frac{a}{h}\right)$ is the non-dimensional crack configuration function, and h is the total strip length (see Fig. 10b).

The local flexibility due to the crack for a unit width strip can be written as

$$c_{ij} = \frac{\partial u_i}{\partial P_j} = \frac{\partial^2}{\partial P_i \partial P_j} \int_0^a J(y)\, dy, \tag{12}$$

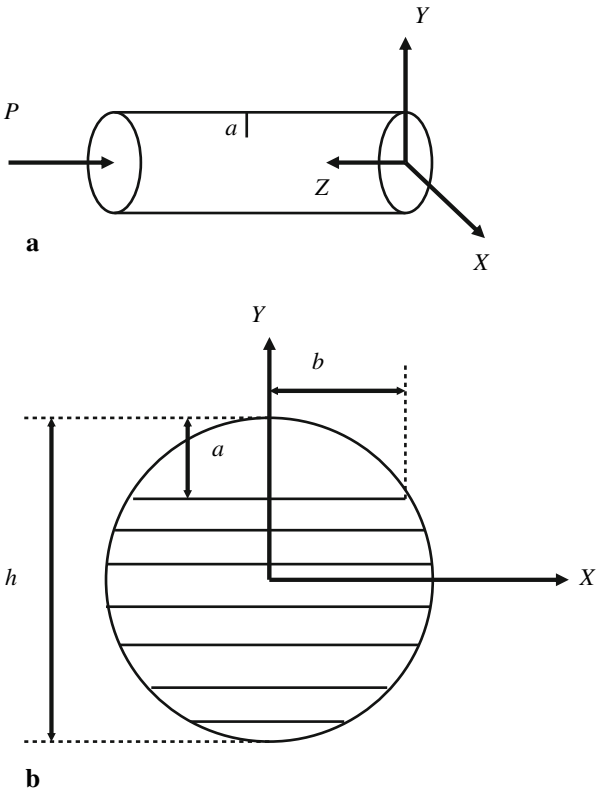

Fig. 10. Local crack model: **a** column section containing a crack; **b** crack cross section

which, after integration along the crack edge, becomes

$$C_{ij} = \frac{\partial^2}{\partial P_i \partial P_j} \int_{-b}^{b} \int_{0}^{a} J(y)\, dy\, dz. \tag{13}$$

In this study the concentric vertical load is only considered, hence C_{11} is required in Eq. (12). The mode I fracture parameter is the only dominating case in this study. Therefore the mode I stress intensity factor is considered.

A dimensionless flexibility factor is defined, $\overline{C_{11}}$, here by normalizing the local flexibility of C_{11}, which can be written as

$$\overline{C_{11}} = C_{11} \frac{\pi E h}{(1-\upsilon^2)}, \tag{14}$$

where C_{11} is obtained using Eq. (12).

The corresponding cracks configuration functions, $F_1(a/h)$ for prismatic columns of rectangular and circular cross section, with a single and double edge cracks can be written as suggested in Ref. [15]:
for rectangular cross section with a single edge crack:

$$F_1(a/h) = \sqrt{\frac{\tan\lambda}{\lambda}}\Big[0.752 + 2.02(a/h) + 0.37(1-\sin\lambda)^3\Big] / \cos\lambda \quad \text{where } \lambda = \frac{\pi a}{2h}; \tag{15}$$

for rectangular cross section with a double edge cracks:

$$F_1\Big(\frac{a}{h}\Big) = \left[1.12 + 0.43\Big(\frac{a}{h}\Big) - 4.79\Big(\frac{a}{h}\Big)^2 + 15.46\Big(\frac{a}{h}\Big)^3\right]; \tag{16}$$

for circular cross section with a double edge cracks:

$$F_1\Big(\frac{\alpha}{h}\Big) = \left[\frac{1.121 - 1.302\big(\frac{\alpha}{h}\big) + 0.988\big(\frac{\alpha}{h}\big)^2 - 0.308\big(\frac{\alpha}{h}\big)^3}{\sqrt{\Big(1-\big(\frac{\alpha}{h}\big)^3\Big)}}\right]. \tag{17}$$

The dimensionless local flexibility $\overline{C_{11}}$ for different crack configuration functions can be obtained by numerically integrating Eqs. (12), (13). As a typical example, for a prismatic column of rectangular cross section with a single edge crack we have

$$\begin{aligned} C_{11} &= \int_0^x \tau(1.12 - 0.23\tau + 10.6\tau^2 - 21.7\tau^3 + 30.4\tau^4)^2 \mathrm{d}\tau \\ &= 92.416x^2(0.555 + (-1.181 + x)x)(0.563 + (-0.880 + x)x)(0.159 + x(0.085 + x)) \\ &\quad (0.135 + x(0.389 + x)), \quad \text{where} \quad x = a/h. \end{aligned} \tag{18}$$

The variation of local flexibility with respect to the normalized crack depth is shown in Fig. 11. Both results obtained from FEM and J-Integral are presented.

It is seen that there is good agreement between the results obtained from the FE method and those obtained from the J-Integral when $a/h \leq 0.55$.

The variation of local flexibility, obtained from the FEM and J-Integral method, with respect to the normalized crack depth, is shown in Fig. 12 for the rectangular and circular cross section of double edge cracked components.

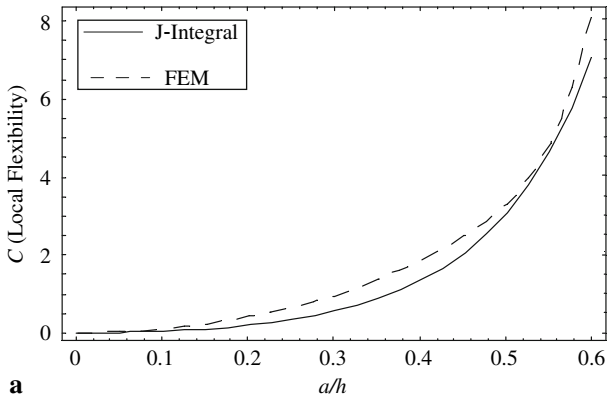

a

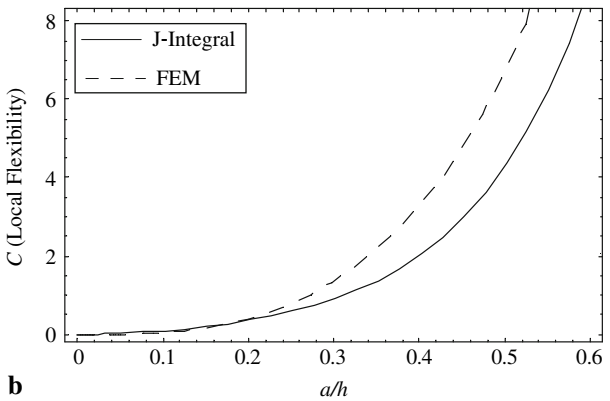

b

Fig. 11. The variation of C, obtained by FEM and J-integral, with a/h for rectangular cross section; **a** single crack, **b** double cracks

It is worth noting that the results obtained for the local flexibility, illustrated in Figs. 11 and 12, are not reliable when $a/h \geq 0.65$ because it was found, for example for a column of rectangular cross section with a single edge crack, that fast fracture phenomena occur if the normalized critical crack depth $a_c/h \geq 0.55$. It was also found that for all different columns geometries and crack types the phenomena of fast fracture occur when $a_c/h \geq 0.45$. Equations (10) and (14)–(18) can be used to estimate the critical normalized crack depth (a_c/h), in which the fast fracture phenomenon occurs. For example, for a rectangular cross section cracked column with a single edge crack equation (10) becomes

$$K_{\mathrm{I}} = \sigma\sqrt{\pi a} F_1\left(\frac{a}{h}\right). \tag{19}$$

We replace K_{I} with the column material fracture toughness constant K_{Ic} as

$$K_{\mathrm{Ic}} = \sigma\sqrt{\pi a_c} F_1\left(\frac{a_c}{h}\right), \tag{20}$$

where $F_1\left(\frac{a_c}{h}\right)$ is determined from Eq. (14). The critical normalized crack length can be calculated from Eq. (19) for the given geometry column. If was found that for all geometries considered the critical normalized crack depth is equal or greater than 0.45 (i.e. $a_c/h \geq 0.45$).

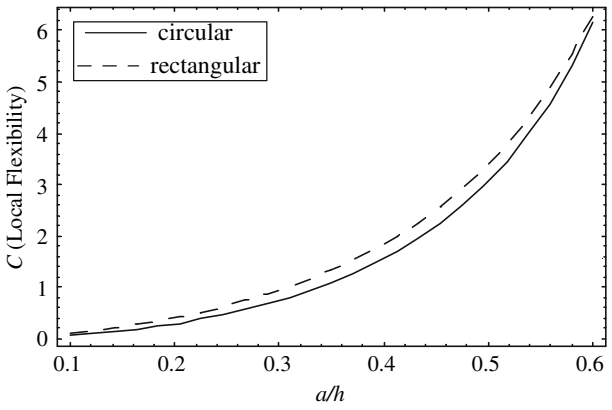

Fig. 12. The variation of C with a/h for rectangular and circular cross section with a single edge crack

4 Buckling analysis of a cracked column

In this Section, using the transfer matrix method and fundamental solution of an intact column, buckling analysis of slender prismatic columns of rectangular and circular cross sections, with a single and double edge cracks, is performed. The transfer matrix method, suggested in Ref. [10], is an efficient and attractive tool for the solution of the eigenvalue problem for one-dimentional structures with nonuniform mechanical properties.

It can be seen from Fig. 2 that the column is divided into segments, segment 1 ($0 \le x \le x_c$) and segment 2 ($x_c \le x \le L$), by the rotational spring. The Euler–Bernoulli beam model will be employed to formulate the governing equation and the following second-order differential equation relating the curvature and moment will be used:

$$\mathrm{EI}\frac{\mathrm{d}^2 y(x)}{\mathrm{d}x^2} = -M(x), \tag{21}$$

where EI is the flexural stiffness of the column. In this case, the relationship among the displacement ($y(x)$), slope ($\theta\ (x)$), bending moment ($M(x)$), and shear force ($V(x)$) are as follows. The relevant displacement and rotation for segments 1 and 2 are expressed here as ($y_1(x)$, $\theta_1(x)$) and ($y_2(x)$, $\theta_2(x)$), respectively,

$$\begin{aligned} \theta_1(x) &= \frac{\mathrm{d}y_1}{\mathrm{d}x}, \\ M_1(x) &= -\mathrm{EI}\frac{\mathrm{d}^2 y_1}{\mathrm{d}x^2}, \\ V_1(x) &= \frac{\mathrm{d}M_1}{\mathrm{d}x} - p\frac{\mathrm{d}y_1}{\mathrm{d}x}. \end{aligned} \tag{22}$$

The differential equation for buckling of segment 1 can be written as [1]

$$\frac{\mathrm{d}^4 y_1}{\mathrm{d}x^4} + k^2\frac{\mathrm{d}^2 y_1}{\mathrm{d}x^2} = 0 \quad \text{where} \quad k^2 = \frac{p}{EI}. \tag{23}$$

The general solution of Eq. (21) is given by

$$y_1(x) = A_1 + A_2 x + A_3 \sin(kx) + A_4 \cos(kx). \tag{24}$$

Using Eqs. (21) and (23), the following relationship can be written:

$$\begin{Bmatrix} y(x) \\ \theta(x) \\ M(x) \\ V(x) \end{Bmatrix} = [B(x)] \begin{Bmatrix} A_1 \\ A_2 \\ A_3 \\ A_4 \end{Bmatrix}, [B(x)] = \begin{bmatrix} 1 & x & \sin(kx) & \cos(kx) \\ 0 & 1 & k\cos(kx) & -k\sin(kx) \\ 0 & 0 & p\sin(kx) & p\cos(kx) \\ 0 & -p & 0 & 0 \end{bmatrix}. \tag{25}$$

The relationship between the parameters written above at the two ends of segment 1 can be expressed as

$$\begin{Bmatrix} y_1(x_c) \\ \theta_1(x_c) \\ M_1(x_c) \\ V_1(x_c) \end{Bmatrix} = [T_1] \begin{Bmatrix} y_1(0) \\ \theta_1(0) \\ M_1(0) \\ V_1(0) \end{Bmatrix} \Rightarrow [T_1] = [B(x_c)][B(0)]^{-1}. \tag{26}$$

$[T_1]$ is called the ''transfer matrix'' for segment 1, because this matrix transfer the parameters at the upper end ($x = 0$) to those at the lower end ($x = x_c$) of segment 1. Similarly for segment 2, $[T_2] = [B(L)]\ [B(x_c)]$, where $[T_2]$ transfer the parameters at ($x = x_c$) to those at ($x = L$) of segment 2. There is continuity among the displacement, bending moment and shear force, at the boundary of segments 1 and 2, but there is a discontinuity between slopes at this point. Caused by the bending moment and rotation of the spring representing the cracked section, as shown in Fig. 13,

$$\begin{aligned} &y_1(x_c) = y_2(x_c), \\ &y_1''(x_c) = y_2''(x_c), \\ &y_1'''(x_c) = y_2'''(x_c), \\ &\theta_2(x_c) - \theta_1(x_c) = y_2'(x_c) - y_1'(x_c) = -CM(x_c). \end{aligned} \tag{27}$$

Equation (26) can be written in matrix form as

$$\begin{Bmatrix} y_2(x_c) \\ \theta_2(x_c) \\ M_2(x_c) \\ V_2(x_c) \end{Bmatrix} = [T_c] \begin{Bmatrix} y_1(x_c) \\ \theta_1(x_c) \\ M_1(x_c) \\ V_1(x_c) \end{Bmatrix}, \quad [T_c] = \begin{bmatrix} 1 & 0 & 0 & \\ 0 & 1 & -C & 0 \\ 0 & 0 & 1 & 0 \\ 0 & 0 & 0 & 1 \end{bmatrix}. \tag{28}$$

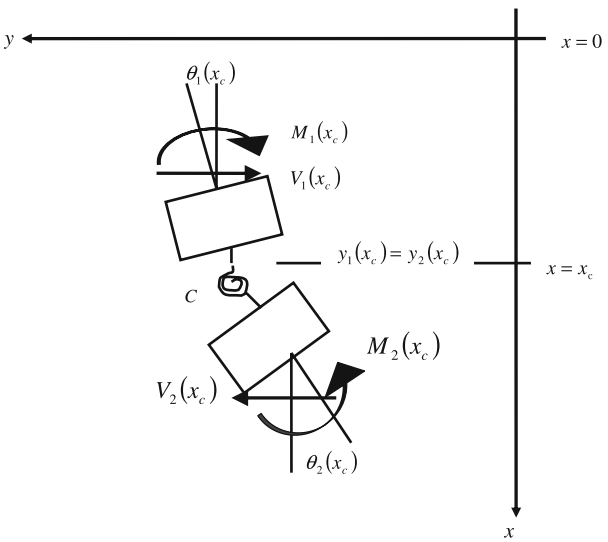

Fig. 13. Boundary conditions for segments 1 and 2

$[T]$ is called the ''general transfer matrix'' that transfers the parameters at the upper end ($x = 0$) of segment 1 to those at the lower end ($x = L$) of segment 2 and can be obtained from Eqs. (25) and (27) as

$$[T] = [T_1][T_c][T_2] = \begin{bmatrix} T_{11} & T_{12} & T_{13} & T_{14} \\ T_{21} & T_{22} & T_{23} & T_{24} \\ T_{31} & T_{32} & T_{33} & T_{34} \\ T_{41} & T_{42} & T_{43} & T_{44} \end{bmatrix}. \tag{29}$$

4.1 Eigenvalue equations and eigenvalues

Eigenvalue equations can be established by using Eq. (29) and the end conditions as follows:

(a) Pinned–pinned ended column: for this case, Eq. (29) becomes

$$\begin{Bmatrix} 0 \\ \theta_2(L) \\ 0 \\ V_2(L) \end{Bmatrix} = \begin{bmatrix} T_{11} & T_{12} & T_{13} & T_{14} \\ T_{21} & T_{22} & T_{23} & T_{24} \\ T_{31} & T_{32} & T_{33} & T_{34} \\ T_{41} & T_{42} & T_{43} & T_{44} \end{bmatrix} \begin{Bmatrix} 0 \\ \theta_1(0) \\ 0 \\ V_1(0) \end{Bmatrix} \Rightarrow \begin{Bmatrix} 0 \\ 0 \end{Bmatrix}$$

$$= \begin{bmatrix} T_{12} & T_{14} \\ T_{32} & T_{34} \end{bmatrix} \begin{Bmatrix} \theta_1(0) \\ V_1(0) \end{Bmatrix} \Rightarrow T_{12}T_{34} - T_{14}T_{32} = 0. \tag{30}$$

It can be seen that the eigenvalues are obtained from a second order determinant.

Following the same procedure, the eigenvalue equations for other boundary conditions are obtained as

(b) Fixed–free

$$T_{11}T_{22} - T_{12}T_{21} = 0; \tag{31}$$

(c) Fixed–pinned

$$T_{12}T_{24} - T_{14}T_{22} = 0; \tag{32}$$

(d) Fixed–fixed

$$T_{13}T_{24} - T_{14}T_{23} = 0; \tag{33}$$

4.2 Critical buckling load

After determining the elements T_{ij} of the matrix $[T]$ and then using Eqs. (30)–(33), the eigenvalue equations are obtained in explicit form as

(a) Pinned–pinned ended column

$$\sin(kL) - Ck \sin(\beta kL) \sin[(1-\beta)kL] = 0; \tag{34}$$

(b) Fixed–free ended column

$$\cos(kL) - Ck \sin(\beta kL) \cos[(1-\beta)kL] = 0; \tag{35}$$

(c) Fixed–pinned ended column

$$[(kL)\cos(kL) - \sin(kL)] + Ck\sin(\beta kL)\{\sin[(1-\beta)kL] - (kL)\cos[(1-\beta)kL]\} = 0; \tag{36}$$

(d) Fixed–fixed ended column

$$\begin{aligned} &4\sin(kL/2)[\sin(kL/2) - (kL/2)\cos(kL/2)] \\ &\quad + Ck\{\sin(kL) - (kL)\cos(\beta kL)\cos[(1-\beta)kL]\} = 0. \end{aligned} \tag{37}$$

In Eqs. (34)–(37), $\beta = x_c/L$ (see Fig. 1) and $k^2 = P/\mathrm{EI}$. By using any of a number of root finder algorithms, the roots (eigenvalues) of the above transcendental equations can be obtained. It is worth nothing that, by setting $C = 0$ in the above equations, one obtains the buckling conditions, i.e. eigenvalue equations, of the corresponding intact columns.

5 Numerical results and discussion

In order to illustrate the proposed method a buckling analysis of a prismatic column with a single and a double edge crack with rectangular and circular cross section is presented.

5.1 A rectangular cross section cracked column with a single edge crack

As a first example, a pinned–pinned column with the following data is considered:

$$\begin{aligned} &E = 200\,\mathrm{GPa},\ a = 0.3h = 9\,\mathrm{cm},\ b = h = 30\,\mathrm{cm}, \\ &L = 3\,\mathrm{m},\ x_c = 0.7L = 2.1\,\mathrm{m} \\ &\quad \Rightarrow \zeta = a/h = 0.3 \Rightarrow C = 0.166968/\mathrm{EI} \\ &\quad \Rightarrow P_{\mathrm{cr}} = 1.0187\mathrm{EI}, \quad P_{\mathrm{e}}\frac{\pi^2\mathrm{EI}}{L^2} = 1.0966\mathrm{EI} \quad \text{where } P_{\mathrm{e}} \text{ is the Euler buckling load.} \end{aligned}$$

Therefore the crack causes 7.1% reduction in the buckling load. The variation of $P_{\mathrm{cr}}/P_{\mathrm{e}}$, versus crack location parameter is shown in Fig. 14. According to the figure when the crack shifts towards any of the supports, its effect diminishes.

In order to see more clearly the effect of the crack depth ($a = \zeta\, h$) and the location ($x_c = \beta\, L$), consider four compression columns having a single non-propagating edge crack and pinned–pinned, fixed–free, fixed–pinned and fixed–fixed support conditions and the same cross sectional dimensions

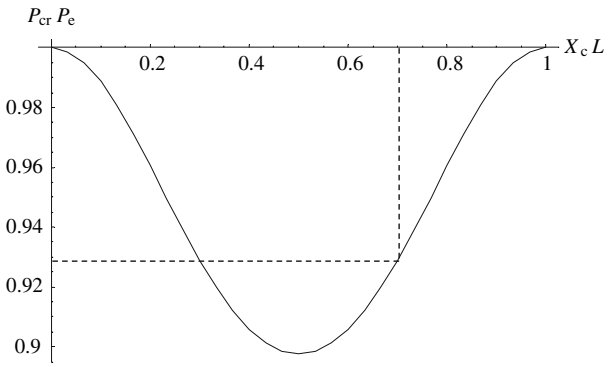

Fig. 14. The variation of $P_{\mathrm{cr}}/P_{\mathrm{e}}$ versus the crack location parameter ($\beta = X_c/L$)

of $h = 0.1$ m, $b = 0.1$ m, but different lengths of 1.30, 0.65 1.85 and 2.60 m, respectively. With these properties all columns buckle in the elastic range. The first critical buckling load to the Euler buckling load $\left(P_{\mathrm{e}} = \frac{\pi^2 \mathrm{EI}}{L^2}\right)$ ratio versus crack location parameter curves, corresponding to the 0.1, 0.25 and 0.45 values of the crack depth parameter, are shown in Fig. 15.

It is clear from the figure that for all columns, when the crack depth and thus the local flexibility increases, the buckling load and thus the $P_{\mathrm{cr}}/P_{\mathrm{e}}$ ratio decreases, as expected. While the largest decrease occurs in the fixed–free ended column, the smallest decrease is in the fixed–fixed column, both for $\zeta = 0.45$. The crack location has different effects depending on the end conditions. As is well known from fracture mechanics and strength of materials, the strain energy stored in an elastic body under a bending effect is directly related to the magnitude of the bending moment. Therefore, for a constant crack depth, a crack located in the section of maximum bending moment causes the largest decrease in the buckling load. Naturally, a crack located in the inflexion point (zero moment point) has no effect on the critical buckling load.

5.2 Critical buckling loads of columns having a single and a double edge crack with rectangular cross sections

As a second example, consider two columns having the fixed–free and pinned–pinned end conditions with the same dimension properties $h = b = 0.1$ m, $L = 1$ m and the dimensionless crack depth $\zeta = 0.15, 0.45$. The variation of $P_{\mathrm{cr}}/P_{\mathrm{e}}$, versus the crack location parameter for these two columns is

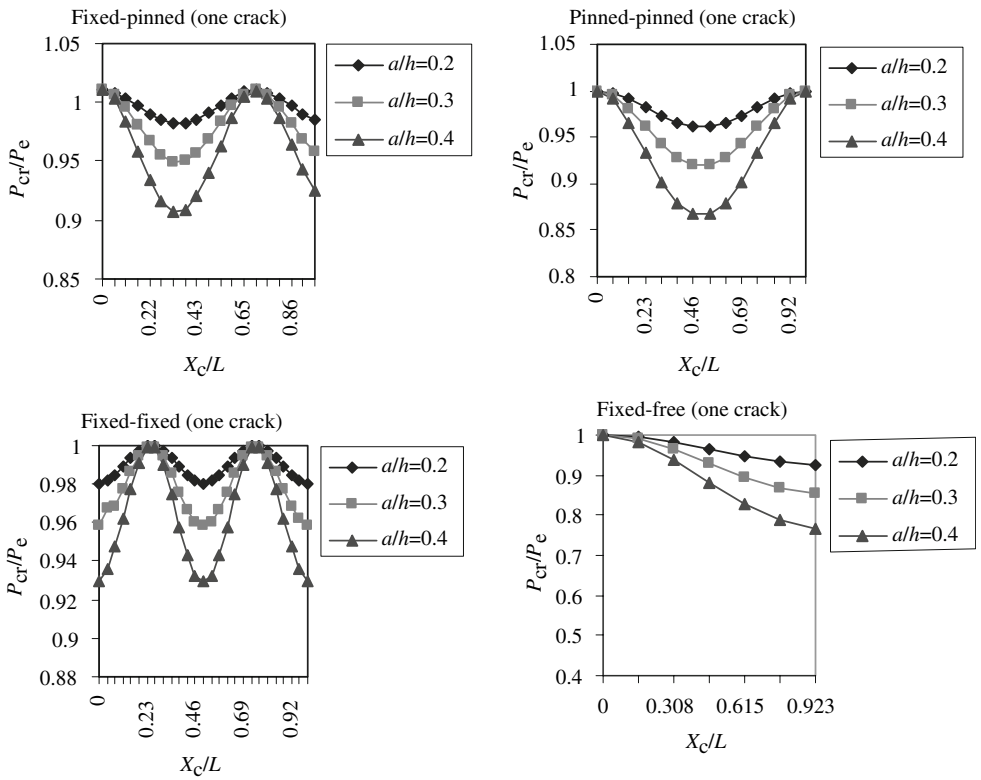

Fig. 15. Variation of the first critical buckling load to the Euler buckling load ratio ($P_{\mathrm{cr}}/P_{\mathrm{e}}$) depending on the dimensionless crack depth ($\zeta = a/h$) and dimensionless crack location ($\beta = X_{\mathrm{c}}/L$)

shown in Fig. 16. As is seen double edge cracks have the larger local flexibility and thus greater decrease the critical buckling load.

5.3 *Critical buckling loads of columns with a single and a double edge crack and circular cross sections*

As a third example, consider two columns having the fixed–free and fixed–pinned end conditions with the same dimension properties $D = h = b = 0.1$ m, $L = 1$ m and the dimensionless crack depth $\zeta = 0.15, 0.45$. The variation of P_{cr}/P_e, versus the crack location parameter for these two columns is shown in Fig. 17. As is seen double edge cracks have the larger local flexibility and thus greater decrease the critical buckling load, but the decrease in the critical buckling load for a circular cross section is smaller than for the rectangular cross section.

5.4 *Critical buckling loads of columns with a double edge crack, having rectangular and circular cross sections*

As the last example, a pinned–pinned (simply supported) column having a single and a double crack with rectangular and circular cross section is considered. For theses columns $h = b = D = 0.2$ m, $L = 2$ m and $\zeta = a/h = 0.2, 0.4$. The results are shown in Fig. 18.

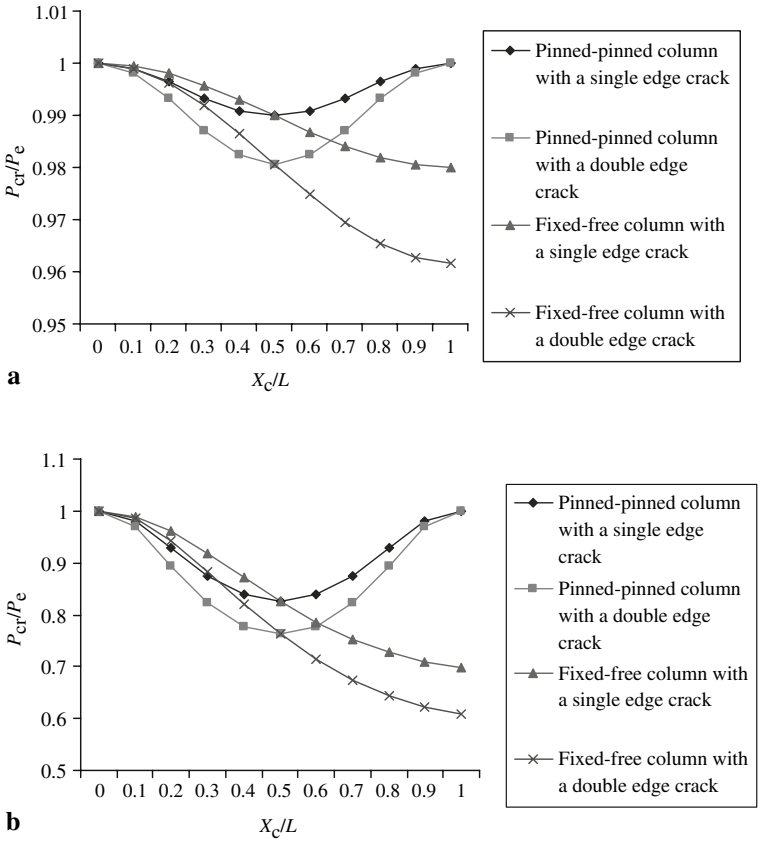

Fig. 16. The variation of P_{cr}/P_e versus the crack location parameter for columns having a single and a double edge crack with rectangular cross section; **a** $a/h = 0.15$, **b** $a/h = 0.45$

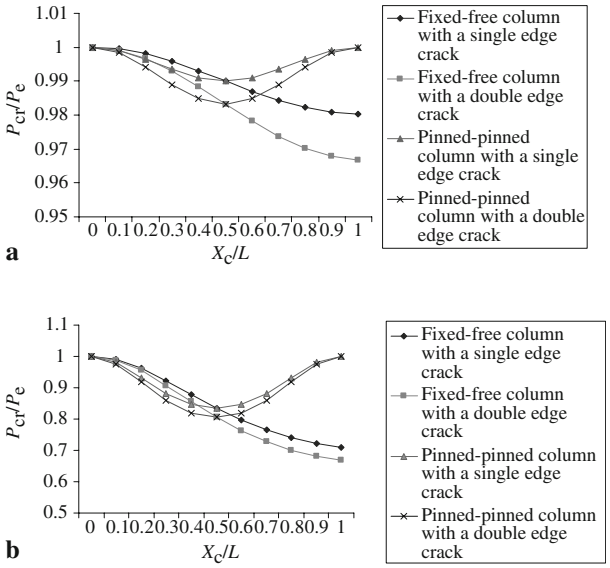

Fig. 17. The variation of P_{cr}/P_e, versus the crack location parameter for columns having a single and a double edge crack with circular cross section; **a** *a/h* = 0.15, **b** *a/h* = 0.45

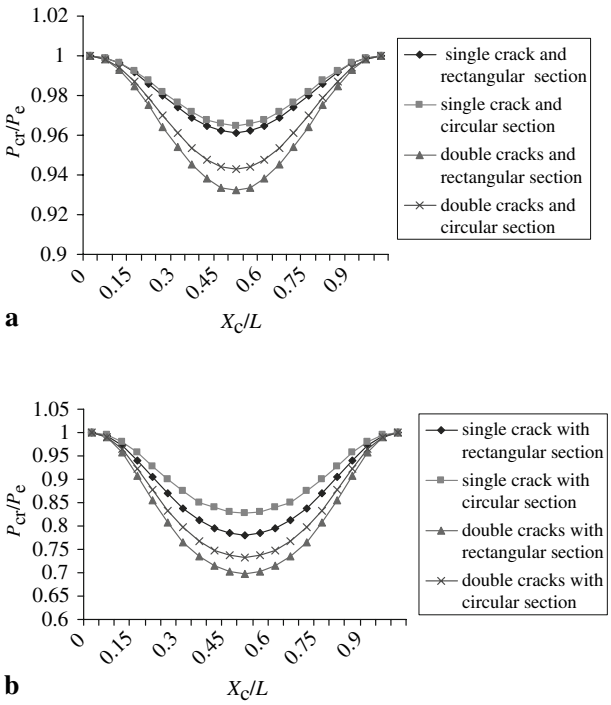

Fig. 18. The variation of P_{cr}/P_e versus crack location parameter for columns having a single and a double edge crack with circular and rectangular cross sections; **a** *a/h* = 0.2, **b** *a/h* = 0.4

6 Conclusions

The buckling analysis of slender prismatic columns of rectangular and circular cross section, with a single and double edge cracks, subjected to concentrated vertical loads has been presented in this study.

Some principal conclusions can be drawn as follows:

(i) Local flexibility functions due to the presence of one and double non-propagating edge cracks in circular and rectangular cross sections are derived. The explicit formulae are obtained and the best-fitted polynomials are also presented.
(ii) There was very good agreement between the flexibility results obtained by finite element and J-Integral approaches (maximum discrepancy less than 2%).
(iii) The effect of a crack on the buckling load of a column depends on the depth and the location of the crack.
(iv) In columns under axial compression, the effect of a crack is to decrease the buckling load. As expected, the load carrying capacity decreases as the crack depth increases. On the other hand, the effect of crack location depends on the end conditions of the column. Generally, the maximum decrease of the buckling capacity occurs when the crack is located at the position with maximum curvature of the buckling mode shape of the column. If a crack is located just in the inflexion points of the corresponding intact column, it has no effect on the buckling load.
(v) The results showed that the buckling capacity obtained for columns having rectangular cross section of $b \times b$ mm^2 is lower than those obtained for a similar column of circular section with a diameter of b mm^2.
(vi) As it is expected, the capacity of columns having a single edge crack is higher than those with double edge cracks.
(vii) The transfer matrix method is a simple and efficient method to analyze the buckling of cracked columns with various boundary conditions. Eigenvalue equations of cracked columns could be easily established from a system of two linear equations.

References

[1] Timoshenko, S.P., Gere, J.M.: Theory of elastic stability. Singapore: Mc Graw-Hill 1961
[2] Euler, L.: Additamentum, ''De curvis elasticis''. In: Methodus inveniendi lineas curevas maximi minimive proprietate gaudentes, Lausanne (1744)
[3] Krawczuk, M., Ostachowicz, W.M.: Modeling and vibration analysis of a cantilever composite beam with a transverse open crack. J. Sound Vibr. **183**, 69–89 (1995)
[4] Liebowitz, H., Vanderveldt, H., Harris, D.W.: Carrying capacity of notched columns. Int. J. Solids Struct. **3**, 489–500 (1967)
[5] Liebowitz, H., Claus, W.D. Jr: Failure of notched columns. Engng. Fract. Mech. **1**, 379–383 (1968)
[6] Okamura, H., Liu, H.W., Chu, C.S.: A cracked column under compression. Engng. Fract. Mech. **1**, 547–564 (1969)
[7] Anifantis, N., Dimarogonas, A.: Stability of columns with a single crack subjected to follower and vertical loads. Int. J. Solids Struct. **19**, 281–291 (1983)
[8] Nikpour, K.: Buckling of cracked composite columns. Int. J. Solids Struct. **26**, 1371–1386 (1990)
[9] Li, Q.S.: Buckling of multi-step cracked columns with shear deformation. Engng. Struct. **23**, 356–364 (2001)
[10] Gurel, M.A., Kisa, M.: Buckling of slender prismatic column with a single edge crack under concentric vertical loads. Turk. J. Engng. Environ. Sci. **29**, 185–193 (2005)
[11] Shifrin E.I., Ruotolo R.: Natural frequencies of a beam with an arbitrary number of cracks. J. Sound Vibr. **222**, 409–23
[12] Fan, S.C., Zheng, D.Y.: Stability of a cracked Timoshenko beam-column by modified Fourier series. J. Sound Vibr. **264**, 475–484 (2003)
[13] Zheng, D.Y., Fan, S.C.: Vibration and stability of cracked hollow-sectional beams. J. Sound Vibr. **267**, 933–954 (2003)
[14] Ansys Level 6.1, Data Preparation Manual, ANSYS, Canonsburg, Pennsylvania (1973)

[15] Tada, H., Paris, P.C., Irwin, G.R.: The stress analysis of cracks handbook, 2nd edn. St. Louis, Paris Productions 1985
[16] Dimarogonas, A.D., Papadopoulos, C.A.: Vibration of cracked shafts in bending. J. Sound Vibr. **91**, 583–593 (1983)